Effect of crystallization water on the structural and electrical properties of CuWO4 under high pressure

Li Wang, Feng Ke, Qinglin Wang, Jiejuan Yan, Cailong Liu, Xizhe Liu, Yanchun Li, Yonghao Han, Yanzhang Ma , and Chunxiao Gao

Citation: Applied Physics Letters **107**, 201603 (2015); doi: 10.1063/1.4935978
View online: http://dx.doi.org/10.1063/1.4935978
View Table of Contents: http://scitation.aip.org/content/aip/journal/apl/107/20?ver=pdfcov
Published by the AIP Publishing

APPLIED PHYSICS LETTERS **107**, 201603 (2015)

Effect of crystallization water on the structural and electrical properties of $CuWO_4$ under high pressure

Li Wang,[1] Feng Ke,[2] Qinglin Wang,[2] Jiejuan Yan,[1] Cailong Liu,[1] Xizhe Liu,[1] Yanchun Li,[3] Yonghao Han,[1,a)] Yanzhang Ma,[2,4] and Chunxiao Gao[1,a)]
[1]*State Key Lab for Superhard Materials, Institute of Atomic and Molecular Physics, Jilin University, Changchun 130012, China*
[2]*Center for High Pressure Science and Technology Advanced Research, Shanghai 201203, China*
[3]*Beijing Synchrotron Radiation Facility, Institute of High Energy Physics, Chinese Academy of Science, Beijing 100049, China*
[4]*Department of Mechanical Engineering, Texas Tech University, Lubbock, Texas 79409, USA*

(Received 27 August 2015; accepted 2 November 2015; published online 17 November 2015)

The effect of crystallization water on the structural and electrical properties of $CuWO_4$ under high pressure has been investigated by *in situ* X-ray diffraction and alternating current impedance spectra measurements. The crystallization water was found to be a key role in modulating the structural stability of $CuWO_4$ at high pressures. The anhydrous $CuWO_4$ undergoes two pressure-induced structural transitions at 8.8 and 18.5 GPa, respectively, while $CuWO_4{\cdot}2H_2O$ keeps its original structure up to 40.5 GPa. Besides, the crystallization water makes the electrical transport behavior of anhydrous $CuWO_4$ and $CuWO_4{\cdot}2H_2O$ quite different. The charge carrier transportation is always isotropic in $CuWO_4{\cdot}2H_2O$, but anisotropic in the triclinic and the third phase of anhydrous $CuWO_4$. The grain resistance of $CuWO_4{\cdot}2H_2O$ is always larger than that of anhydrous $CuWO_4$ in the entire pressure range. By analyzing the relaxation response, we found that the large number of hydrogen bonds can soften the grain characteristic frequency of $CuWO_4{\cdot}2H_2O$ over $CuWO_4$ by one order of magnitude. © *2015 AIP Publishing LLC*. [http://dx.doi.org/10.1063/1.4935978]

Crystallization water exists in the crystalline framework of some metal complex or inorganic salts and is not directly bonded to the metal cations. At ambient pressure, the crystallization water can be removed by heating, which results in considerable differences in physical and mechanical properties between the anhydrous and the hydrated salts.[1–3] For example, compared with the luminescence of anhydrous magnesium tungstate ($MgWO_4$), hydrated magnesium tungstate ($MgWO_4{\cdot}2H_2O$) has extra emission bands related to the hydrate group.[2] Besides, water can change the physical properties of minerals and rocks, including the plastic deformation, elastic properties,[4–6] electrical properties,[7–13] and structural phase transitions,[14,15] which makes the richness of geologic activity inside the earth. Therefore, studying the effect of crystallization water on the physical and mechanical properties of inorganic salts is a matter of interest in many scientific fields.

As one member of the inorganic salts with crystallization water, metal tungstates and molybdates have been attracting intensive interest for its wide application prospect in scintillation detectors, laser host materials, photoelectrolysis, and optical fibers.[16–19] Their general chemical formula is $ABO_4{\cdot}nH_2O$, where A = (Zn, Mg, Cu, Co), B = (W, Mo), and n = (1, 2, 3). Herein, we select anhydrous copper tungstate ($CuWO_4$) and hydrated copper tungstate ($CuWO_4{\cdot}2H_2O$) as the research objects, aiming to study the effect of crystallization water on the structural and electrical transport properties, and reveal the mechanism behind. At ambient conditions, $CuWO_4$ crystallizes into the triclinic structure with *P*–1 symmetry (distorted wolframite structure),[20] while $CuWO_4{\cdot}2H_2O$ crystallizes into the monoclinic wolframite structure.[21] Under high pressures, the physical properties of $CuWO_4$ have been studied systematically by a variety of experimental methods. Ruiz-Fuertes *et al.* used the optical-absorption measurements to monitor the indirect band-gap under pressure,[22] performed the X-ray diffraction (XRD) and Raman spectra experiments to make *in situ* observation of the structural transition at ~10 GPa and ~17 GPa,[23] and employed the extended X-ray absorption fine structure method to study the electronic structure of $CuWO_4$.[24] Compared with $CuWO_4$, $CuWO_4{\cdot}2H_2O$ has two additional molecules of crystallization water; thus, a large numbers of hydrogen bonds exist in the framework of $CuWO_4{\cdot}2H_2O$. Günter *et al.*, Bars *et al.*, and Le Marouille *et al.* have ever studied the role of hydrogen bonds in the dihydrates $MgWO_4$, $MgMoO_4$, and $ZnMoO_4$, where the hydrogen bonds stabilize the structures under ambient pressure.[1,25,26] Although $CuWO_4{\cdot}2H_2O$ has a similar chemical formula with the dihydrates of $MgWO_4$, $MgMoO_4$, and $ZnMoO_4$, it remained unknown whether or not the crystallization water in $CuWO_4{\cdot}2H_2O$ has the ability to stabilize the structure under high pressure. Besides, the effect of crystallization water on the other physical properties is also a very interesting issue. However, no studies have been conducted to that respect. We believe that such studies will be helpful in establishing a more universal viewpoint on the role of crystallization water in hydrated inorganic salts and minerals and hence they are timely.

In this paper, the crystallization water effect on the structural stability and the electrical transport properties of $CuWO_4$ has been studied by using high-pressure X-ray

a)Authors to whom correspondence should be addressed. Electronic addresses: hanyh@jlu.edu.cn and cc060109@qq.com

diffraction and alternating current (AC) impedance spectroscopy measurements.

High-pressure XRD experiments on $CuWO_4$ and $CuWO_4{\cdot}2H_2O$ were performed at beamline 15U1 of Shanghai Synchrotron Radiation Facility and beamline 4W2 of Beijing Synchrotron Radiation Facility ($\lambda = 0.6199$ Å), respectively. High pressure was generated by a diamond anvil cell (DAC) with an anvil culet of 400 μm in diameter. Silicone oil was used as pressure transmitting medium in $CuWO_4$ experiment. No pressure medium was used in $CuWO_4{\cdot}2H_2O$ experiment. A piece of ruby with 10 μm in size was used as the pressure calibrator.[27] The diffraction images were integrated using the FIT2D program. The Rietveld refinements were carried out using the GSAS program.

Impedance spectra were measured with two-electrode configuration. The experimental details can be found in previous works.[28–30] No pressure-transmitting medium was used in electrical transport measurements for avoiding the introduction of impurities. $CuWO_4{\cdot}2H_2O$ powder with purity of 99.5% was bought from Alfa Aesar Company. Anhydrous $CuWO_4$ was obtained by annealing hydrous $CuWO_4$ at 693 K.[31,32] The anhydrous $CuWO_4$ sample has always been preserved in a glove box since it was dehydrated, and we did load the sample into DAC in the same glove box.

For exploring the crystallization water effect on the structural stability of $CuWO_4$, we conducted high-pressure XRD measurements on both samples. Fig. 1 shows the selected XRD patterns of anhydrous $CuWO_4$ up to 30.1 GPa. During the compression process, all the diffraction peaks below 8.2 GPa can be indexed into the triclinic structure. With further compression up to 8.8 GPa, two new characteristic peaks at 6.5° and 10° can be clearly observed, which indicates the beginning of the phase transition of $CuWO_4$ from the triclinic to the monoclinic structure. Above 18.5 GPa, two additional diffraction peaks appear at 7.3° and 11.7°, indicating that the second structural phase transition occurs. However, the crystal structure of the third phase has not been solved yet. The structural parameters of the triclinic phase at 1.0 GPa and the monoclinic phase at 12.8 GPa obtained by Rietveld refinements are shown in Table I.

TABLE I. Structural parameters of the triclinic and monoclinic structure of anhydrous $CuWO_4$.

Structure	Triclinic $P-1$	Monoclinic $P2/c$
Pressure (GPa)	1.0	12.8
a (Å)	4.6865	4.5763
b (Å)	5.8196	5.5483
c (Å)	4.8764	4.8718
α (°)	91.561	90
β (°)	92.326	87.224
γ (°)	83.256	90

Fig. 2(a) is the selected XRD patterns of $CuWO_4{\cdot}2H_2O$ up to 40.5 GPa. It can be found that no structural phase transition takes place in the whole investigated pressure range, which indicates the structure of $CuWO_4{\cdot}2H_2O$ is stable at high pressure due to the existence of the crystallization water. $CuWO_4{\cdot}2H_2O$ has a similar layer structure with the $MM'O_4{\cdot}2H_2O$ (M = Mg, M' = W, Mo; M = Zn, M' = Mo) as shown in Figs. 2(b) and 2(c), where the $[MO_4(H_2O)_2]$ octahedrons are linked with the $[M'O_4]$ tetrahedrons in the a-b plane, and the neighboring layers are held together by hydrogen bonds with the fourth vertex of the tetrahedron not shared.[1,25,26] Due to the existence of the water molecules, a lot of hydrogen bonds can be generated, which makes the structure of $CuWO_4{\cdot}2H_2O$ more stable at high pressure.

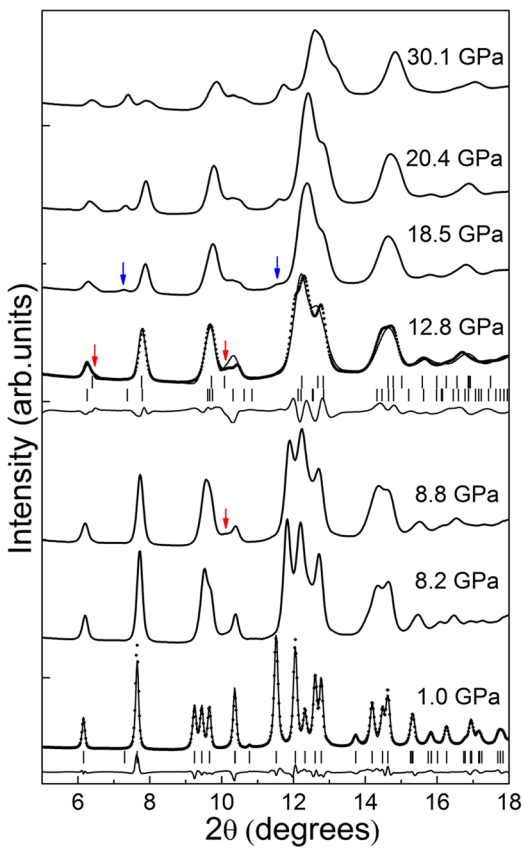

FIG. 1. High pressure XRD spectra of anhydrous $CuWO_4$ at room temperature. Rietveld refinements are shown for the triclinic structure at 1.0 GPa and the monoclinic structure at 12.8 GPa.

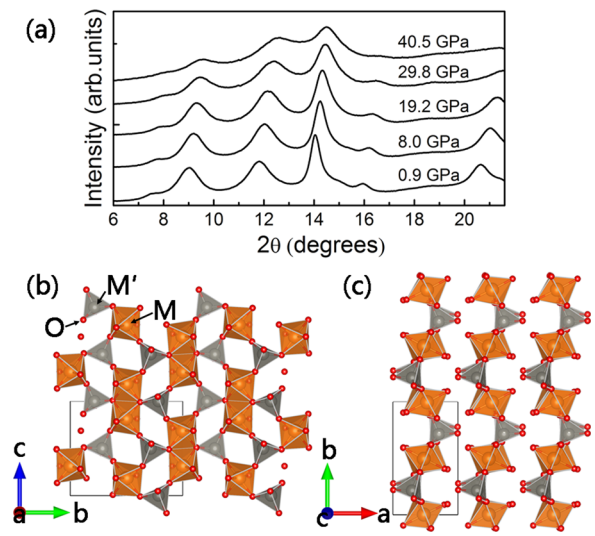

FIG. 2. (a) High pressure XRD spectra of $CuWO_4{\cdot}2H_2O$ with pressure up to 40.5 GPa measured at room temperature. (b) and (c) Projections of the $MM'O_4{\cdot}2H_2O$ structure in different directions.

To study the effect of crystallization water on the electrical transport properties of $CuWO_4$ under high pressure, we conducted the AC impedance spectrum measurements. Figs. 3 and 4 show the typical Nyquist plots and the frequency dependence of imaginary part (Z") for anhydrous $CuWO_4$ and $CuWO_4{\cdot}2H_2O$, respectively. As shown in Fig. 3(a), below 7.7 GPa, two highly overlapped semicircles can be observed, where the left in the high frequency range denotes the grain conduction of $CuWO_4$, and the right in the low frequency range denotes the grain boundary conduction. The grain conduction arc is smaller than the grain-boundary conduction arc, indicating the grain boundary exhibits a larger contribution to the total resistance than the grain. Above 7.7 GPa, only one arc can be observed in the impedance spectra as shown in Fig. 3(c). For example, the conduction of grain and grain boundary cannot be distinguished in the monoclinic phase of $CuWO_4$ as if the grains and the grain boundaries have been "fused" to the transporting charge carriers. With further compression up to 16 GPa, interestingly, the conduction of grain boundaries appears again in the AC impedance spectra as shown in Fig. 3(e). So far, there has not been a proper theory in published literature which can explain the fusion and the separation of the conduction of grain and grain boundary under high pressure. In this paper, we present a model to explain the phenomena described above, where the appearance of the conduction of grain boundary is tentatively related to the anisotropy of the charge carrier transportation in the crystallites. If the electrical transport in a given phase is isotropic, the charge carriers continue along propagation vectors as they cross grain boundaries. In particular, charges will not be scattered off grain boundaries. Therefore, in the Nyquist plot only one semicircle that represents the conduction of grain can be seen, and this is the situation for the monoclinic phase of $CuWO_4$. In contrast, in the case of anisotropic, if the electrical transport is anisotropic, the charges change their propagation vectors along with scattering of grain boundaries in order to follow a minimum energy path in the other adjacent grain, which is the reason why two semicircles can be seen in the triclinic and the new structure of $CuWO_4$.

In the case of $CuWO_4{\cdot}2H_2O$, only one arc is observed in the impedance spectra as shown in Fig. 4. This indicates that the electrical transport in $CuWO_4{\cdot}2H_2O$ is isotropic throughout the examined pressure range.

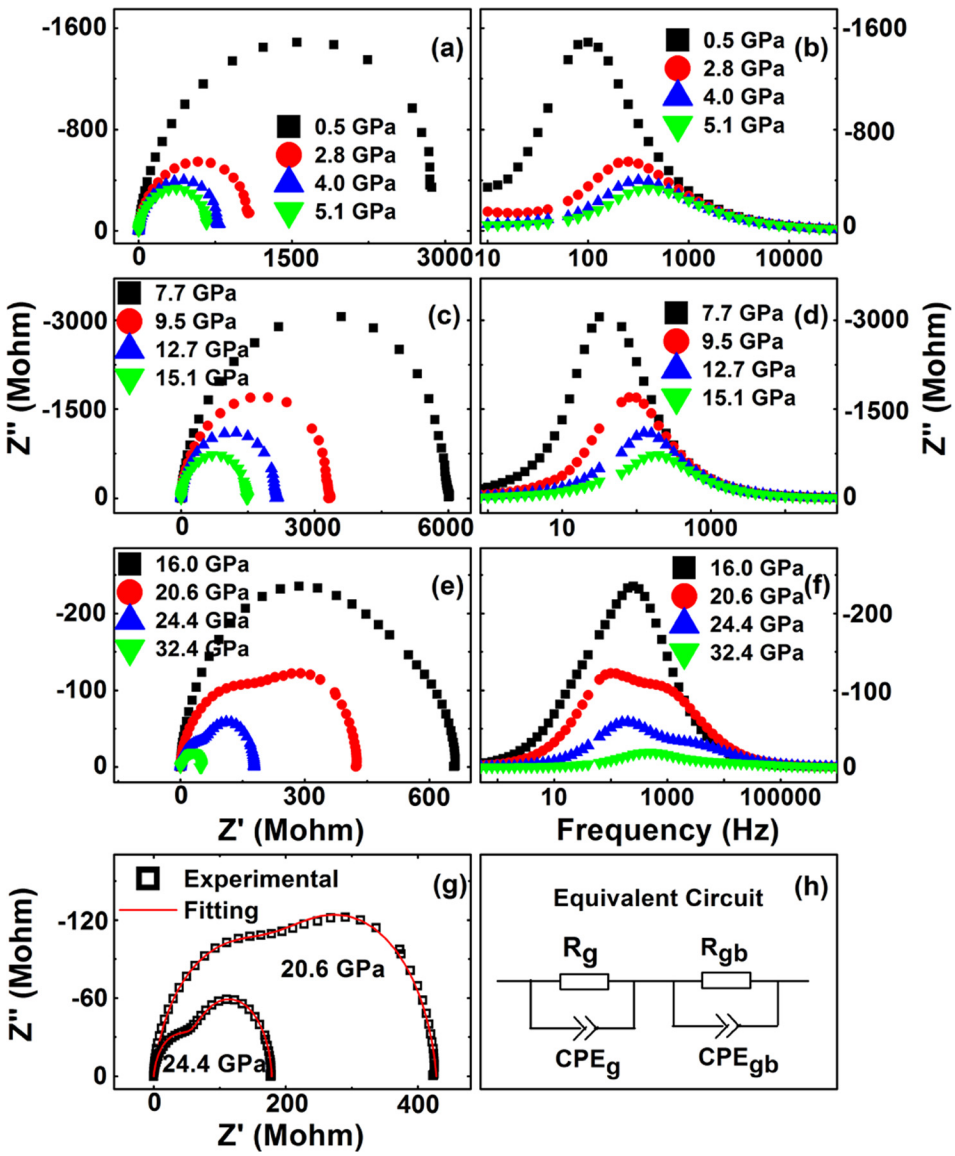

FIG. 3. The Nyquist plots ((a), (c), (e)), and Z"-f ((b), (d), (f)) of the impedance spectra of anhydrous $CuWO_4$ under compression and the fitting results (g) obtained by the equivalent circuit (h).

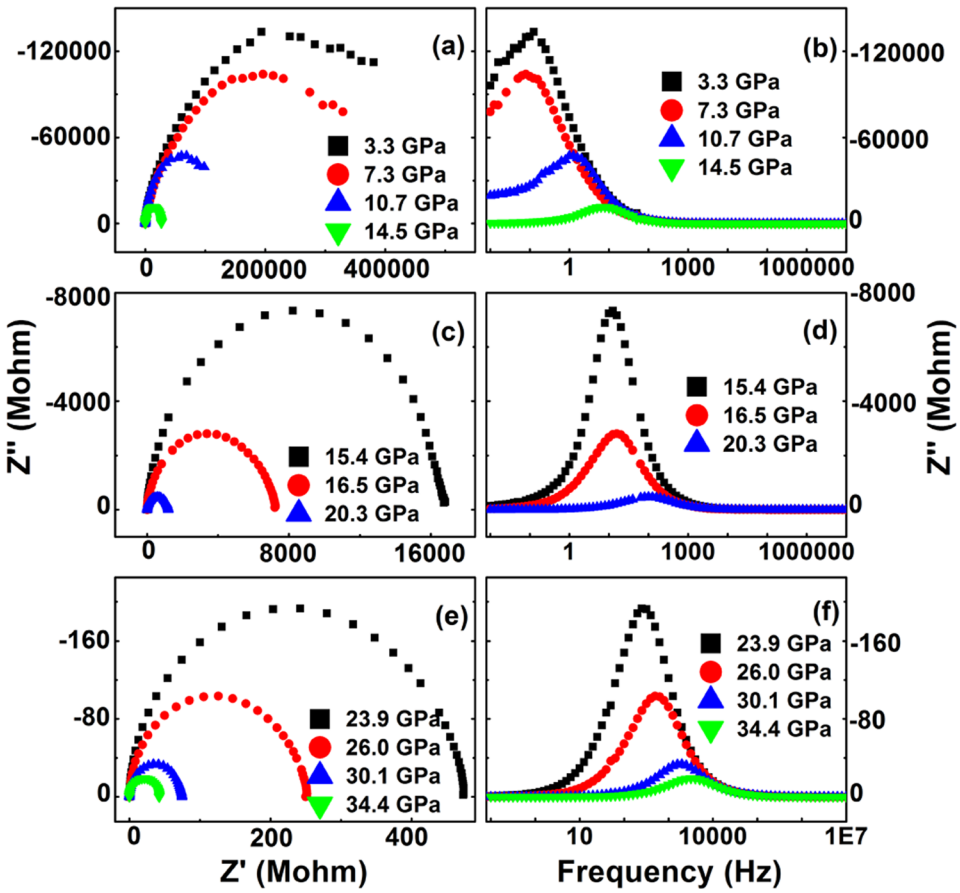

FIG. 4. The Nyquist plots ((a), (c), (e)), and Z″-f ((b), (d), (f)) of the impedance spectra of $CuWO_4{\cdot}2H_2O$ under compression.

To quantify the characteristic relaxation frequencies and the electrical resistances of grains and grain boundaries of $CuWO_4$ and $CuWO_4{\cdot}2H_2O$, we fit the experimental results with an equivalent-circuit method.[33] The fitted results and the equivalent circuit are shown in Figs. 3(g) and 3(h), respectively. The characteristic relaxation frequency can be calculated from the equivalent circuit model according to the following equations:[34,35]

$$C = (RT)^{1/P}/R, \tag{1}$$

$$f = 1/RC, \tag{2}$$

where C is the capacitance, R is the resistance, T and P are the fitting parameters of the constant phase element, and f is the relaxation frequency.

By fitting the impedance spectra, we obtained the pressure dependence of resistance and relaxation frequency for the conduction of grain and the grain boundary as shown in Fig. 5. For anhydrous $CuWO_4$, both of the resistance and the relaxation frequency change noticeably at 7.7 GPa. The effect of grain boundaries starts to emerge above 16.0 GPa. According to our X-ray diffraction measurements, these two changes can be attributed to the structural transitions from triclinic to monoclinic phase and then to a new high-pressure phase. For each phase, the total resistance decreases with increasing pressure, which may be due to large amounts of defects mobilisation caused by structural transition and the narrowing of the band-gap as suggested by Ruiz-Fuertes *et al.* through the optical-absorption measurements.[22] For $CuWO_4{\cdot}2H_2O$, the grain and grain boundary resistance decreases gradually and the relaxation frequency increases with the compression. Due to the crystallization water, the grain resistance of $CuWO_4{\cdot}2H_2O$ is always larger than that of anhydrous $CuWO_4$ in the investigated pressure range. The grain characteristic frequency of $CuWO_4{\cdot}2H_2O$ is lower by at least one order of magnitude than

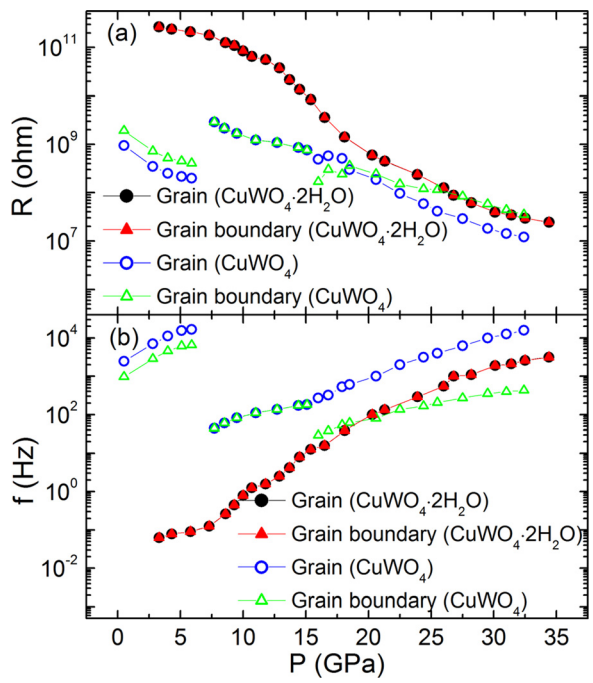

FIG. 5. Pressure dependence of (a) resistance and (b) relaxation frequency for grain and grain boundary of anhydrous $CuWO_4$ and $CuWO_4{\cdot}2H_2O$.

TABLE II. The pressure dependence of the activation energy.

			dH/dP (meV/GPa)	
Sample	Phase	Pressure region (GPa)	Grain	Grain boundary
$CuWO_4$	Triclinic	0.5–5.9	−9.1918	−9.2390
	Monoclinic	7.7–15.1	−4.5668	−4.5668
	New	16.0–32.4	−6.3634	−4.1185
$CuWO_4{\cdot}2H_2O$	Monoclinic	3.3–34.4	−9.8052	−9.8052

that of anhydrous $CuWO_4$ due to a large number of hydrogen bonds.

According to the Arrhenius relationship, the characteristic relaxation frequency can be expressed by the following equation:

$$f = f_0 \exp(-H/k_B T), \tag{3}$$

where H represents the carrier electrical transport activation energy, k_B is the Boltzmann constant, and T is the temperature. Assuming that f and H are the monotropic functions of pressure, and f_0 remains constant, and therefore we have

$$d(\ln f)/dP = -1/k_B T(dH/dP). \tag{4}$$

We obtained the pressure dependence of activation energy, as shown in Table II. In fact, the characteristic relaxation frequency represents the charge-discharge rate in the dipole oscillation process, and its activation energy denotes the energy to activate the resonance.[36] It can be seen clearly that all the activation energies decrease with increasing pressure. This indicates that the vibration damping of W-O dipoles is weakened with increasing pressure and the charge-discharge process becomes easier.[36]

In summary, we have performed the X-ray diffraction and the AC impedance spectra experiments on anhydrous $CuWO_4$ and $CuWO_4{\cdot}2H_2O$ at high pressures. The results indicate that the anhydrous $CuWO_4$ goes through two structural phase transitions at 8.8 and 18.5 GPa, respectively. However, no structural transition takes place on $CuWO_4{\cdot}2H_2O$ with pressure up to 40.5 GPa, indicating that water molecules make the structure of $CuWO_4$ more stable. The grain resistance of $CuWO_4{\cdot}2H_2O$ decreases monotonously with compression and is always larger than that of the anhydrous $CuWO_4$ up to the highest pressure in this measurement, 32.4 GPa. The crystallization water makes the anisotropy (isotropy) of the charge carrier transportation of anhydrous $CuWO_4$ and $CuWO_4{\cdot}2H_2O$ quite different. The $CuWO_4{\cdot}2H_2O$ has lower grain characteristic frequency than that of anhydrous $CuWO_4$ due to a large number of hydrogen bonds. The decrease of activation energies shows that the vibration damping of W-O dipoles is weakened with increasing pressure and the charge-discharge process becomes easier.

This work was supported by the National Basic Research Program of China (Grant No. 2011CB808204), the National Natural Science Foundation of China (Grant Nos. 11374121, 11404133, and 51273079), and the Program of Science and Technology Development Plan of Jilin Province (Grant No. 20140520105JH).

[1]J. R. Günter and E. Dubler, J. Solid State Chem. **65**, 118 (1986).
[2]G. Blasse, G. J. Dirksen, M. Hazenkamp, and J. R. Günter, Mater. Res. Bull. **22**, 813 (1987).
[3]M. Amberg, J. R. Günter, H. Schmalle, and G. Blasse, Solid State Chem. **77**, 162 (1988).
[4]H. Yusa and T. Inoue, Geophys. Res. Lett. **24**, 1831, doi:10.1029/97GL51794 (1997).
[5]T. Inoue, D. J. Weidner, P. A. Northrup, and J. B. Parise, Earth Planet. Sci. Lett. **160**, 107 (1998).
[6]H. Yusa, T. Inoue, and Y. Ohishi, Geophys. Res. Lett. **27**, 413, doi:10.1029/1999GL011032 (2000).
[7]X. Y. Li and R. Jeanloz, Nature **350**, 332 (1991).
[8]X. G. Huang, Y. S. Xu, and S.-i. Karato, Nature **434**, 746 (2005).
[9]T. Yoshino, T. Matsuzaki, S. Yamashita, and T. Katsura, Nature **443**, 973 (2006).
[10]T. Yoshino and T. Katsura, Earth Planet. Sci. Lett. **337–338**, 56 (2012).
[11]X. Z. Guo and T. Yoshino, Earth Planet. Sci. Lett. **369–370**, 239 (2013).
[12]T. Yoshino and T. Katsura, Annu. Rev. Earth Planet. Sci. **41**, 605 (2013).
[13]T. Yoshino, A. Shimojuku, and D. Y. Li, Phys. Earth Planet. Inter. **227**, 48 (2014).
[14]L.-g. Liu, Phys. Earth Planet. Inter. **49**, 142 (1987).
[15]E. Ohtani and K. D. Litasov, Rev. Mineral. Geochem. **62**, 397 (2006).
[16]V. B. Mikhailik and H. Kraus, Phys. Status Solidi B **247**, 1583 (2010).
[17]P. K. Pandey, N. S. Bhave, and R. B. Kharat, Mater. Lett. **59**, 3149 (2005).
[18]J. E. Yourey and B. M. Bartlett, J. Mater. Chem. **21**, 7651 (2011).
[19]J. E. Yourey, K. J. Pyper, J. B. Kurtz, and B. M. Bartlett, J. Phys. Chem. C **117**, 8708 (2013).
[20]L. Kihlborg and E. Gebert, Acta Crystallogr. B **26**, 1020 (1970).
[21]B. Li and F. L. Du, J. Funct. Mater. **4**, 210 (2010) (in Chinese).
[22]J. Ruiz-Fuertes, D. Errandonea, A. Segura, F. J. Manjón, Z. Zhu, and C. Y. Tu, High Pressure Res. **28**, 565 (2008).
[23]J. Ruiz-Fuertes, D. Errandonea, R. Lacomba-Perales, A. Segura, J. González, F. Rodríguez, F. J. Manjón, S. Ray, P. Rodríguez-Hernández, A. Muñoz, Zh. Zhu, and C. Y. Tu, Phys. Rev. B **81**, 224115 (2010).
[24]J. Ruiz-Fuertes, A. Friedrich, J. Pellicer-Porres, D. Errandonea, A. Segura, W. Morgenroth, E. Haussühl, C.-Y. Tu, and A. Polian, Chem. Mater. **23**, 4220 (2011).
[25]J. Y. Le Marouille, O. Bars, and D. Grandjean, Acta Crystallogr. B **36**, 2558 (1980).
[26]O. Bars, J. Y. Le Marouille, and D. Grandjean, Acta Crystallogr. B **37**, 2148 (1981).
[27]H. K. Mao, P. M. Bell, J. W. Shaner, and D. J. Steinberg, J. Appl. Phys. **49**, 3276 (1978).
[28]Y. H. Han, C. X. Gao, Y. Z. Ma, H. W. Liu, Y. W. Pan, J. F. Luo, M. Li, C. Y. He, X. W. Huang, G. T. Zou, Y. C. Li, and J. Liu, Appl. Phys. Lett. **86**, 064104 (2005).
[29]C. Y. He, C. X. Gao, Y. Z. Ma, M. Li, A. M. Hao, X. W. Huang, B. G. Liu, D. M. Zhang, C. L. Yu, G. T. Zou, Y. C. Li, H. Li, X. D. Li, and J. Liu, Appl. Phys. Lett. **91**, 092124 (2007).
[30]Y. Wang, Y. H. Han, C. X. Gao, Y. Z. Ma, C. L. Liu, G. Peng, B. J. Wu, B. Liu, T. J. Hu, X. Y. Cui, W. B. Ren, Y. Li, N. N. Su, H. W. Liu, and G. T. Zou, Rev. Sci. Instrum. **81**, 013904 (2010).
[31]S. M. Montemayor and A. F. Fuentes, Ceram. Int. **30**, 393 (2004).
[32]D. J. Jovanović, I. L. Validžić, M. Mitrić, and J. M. Nedeljković, Acta Chim. Slov. **59**, 70–74 (2012).
[33]Th. Dittrich, J. Weidmann, F. Koch, I. Uhlendorf, and I. Lauermann, Appl. Phys. Lett. **75**, 3980 (1999).
[34]Q. L. Wang, O. Varghese, C. Grimes, and E. Dickey, Solid State Ionics **178**, 187 (2007).
[35]Y. Wang, C. L. Liu, Y. Gao, C. J. Wang, B. Liu, T. J. Hu, W. B. Ren, Y. H. Han, and C. X. Gao, Phys. Status Solidi C **8**, 1687 (2011).
[36]Q. L. Wang, Y. H. Han, C. L. Liu, Y. Z. Ma, W. B. Ren, and C. X. Gao, Appl. Phys. Lett. **100**, 172905 (2012).